

# Dimensionality Dependence of Aging in Kinetics of Diffusive Phase

## Separation: Behavior of order-parameter autocorrelation

Jiarul Midya, Suman Majumder and Subir K. Das\*

*Theoretical Sciences Unit, Jawaharlal Nehru Centre for Advanced*

*Scientific Research, Jakkur P.O., Bangalore 560064, India*

(Dated: June 8, 2021)

Behavior of two-time autocorrelation during the phase separation in solid binary mixtures are studied via numerical solutions of the Cahn-Hilliard equation as well as Monte Carlo simulations of the Ising model. Results are analyzed via state-of-the-art methods, including the finite-size scaling technique. Full forms of the autocorrelation in space dimensions 2 and 3 are obtained empirically. The long time behavior are found to be power-law type, with exponents unexpectedly higher than the ones for the ferromagnetic ordering. Both Chan-Hilliard and Ising models provide results consistent with each other.

PACS numbers: 81.40.Cd, 05.70.Fh, 05.70.Ln

## I. INTRODUCTION

Properties of a nonequilibrium system change with growing age [1]. Understanding of such aging phenomena is of fundamental importance in all branches of science and technology. There have been serious activities on this issue concerning living [2, 3] as well as nonliving matters, especially in problems related to domain growth [1, 4–14] and glassy dynamics [15–19]. Among other quantities, aging phenomena is studied via the two-time autocorrelation function [4]

$$C(t, t_w) = \langle \psi(\vec{r}, t) \psi(\vec{r}, t_w) \rangle - \langle \psi(\vec{r}, t) \rangle \langle \psi(\vec{r}, t_w) \rangle. \quad (1)$$

In Eq. (1),  $\psi$  is a space ( $\vec{r}$ ) and time dependent order parameter,  $t_w$  is the waiting time or age of the system and  $t$  ( $> t_w$ ) is the observation time.

In phase ordering systems [20], though time translation invariance is broken,  $C(t, t_w)$  is expected to exhibit scaling with respect to  $t/t_w$ . Important examples are ordering of spins in a ferromagnet, kinetics of phase separation in a binary ( $A + B$ ) mixture, etc., having been quenched to a temperature ( $T$ ) below the critical value ( $T_c$ ), from a homogeneous configuration. Though full forms are unknown even for very simple models, asymptotically  $C(t, t_w)$  is expected to obey power-law scaling behavior as [4, 6]

$$C(t, t_w) \sim x^{-\lambda}; \quad x = \ell/\ell_w. \quad (2)$$

In Eq. (2),  $\ell$  and  $\ell_w$  are the average sizes of domains, formed by spins or particles of similar type, at times  $t$  and  $t_w$ , respectively. Typically  $\ell$  and  $t$  are related to each other via power-laws.

For nonconserved order-parameter dynamics, e.g., ordering in a ferromagnet, such scaling has been observed and the values of the exponent  $\lambda$  have been accurately estimated [6, 14] in different space dimensions  $d$ . There the exponents follow the bounds

$$\frac{d}{2} \leq \lambda \leq d, \quad (3)$$

predicted by Fisher and Huse (FH) [4]. In kinetics of phase separation in solid mixtures, for which the order parameter is a conserved quantity, the state of understanding is far from satisfactory, due to theoretical as well as computational difficulties. There exist reports [11] of violation of scaling with respect to  $t/t_w$ . The latter observation, our results indicate, is due to the fact that scaling is achieved for  $t_w \gg 1$ . Access to such long time is constrained by inadequate computational resources. This difficulty, in some studies [9, 13], might have led to the conclusion about incorrect values of  $\lambda$ .

In an important work, Young et al. [7] put a more general lower bound on  $\lambda$ , valid irrespective of the conservation of the total order parameter, as

$$\lambda \geq \frac{\beta + d}{2}, \quad (4)$$

where  $\beta$  is the exponent for small wave-vector power-law enhancement of equal time structure factor which, depending upon the dynamics, becomes important for  $t_w \gg 1$ , as stated below. In nonconserved dynamics,  $\beta = 0$  and so the lower bound in Eq. (3) is recovered. For conserved order parameter dynamics, on the other hand,  $\beta = 4$  in both  $d = 2$  and  $3$  at late time. Thus, the upper bound in Eq. (3) is violated. Simulations of the Cahn-Hilliard (CH) equation [20]

$$\frac{\partial \psi(\vec{r}, t)}{\partial t} = -\nabla^2 \left[ \psi(\vec{r}, t) + \nabla^2 \psi(\vec{r}, t) - \psi^3(\vec{r}, t) \right], \quad (5)$$

by Young et al. [7], observed  $\lambda > 3$  in  $d = 2$ , consistent with Eq. (4). From these simulations, the authors, however, did not accurately quantify  $\lambda$ ; scaling of  $C(t, t_w)$  with respect to  $t/t_w$  was not demonstrated; focus was rather on the sensitivity of the aging dynamics to the correlations in the initial configurations. Situation is far worse in  $d = 3$ , with respect to the CH equation as well as the Ising model [1, 20]

$$H = -J \sum_{\langle ij \rangle} S_i S_j; \quad S_i = \pm 1; \quad J > 0. \quad (6)$$

In this paper, we study both CH equation and the Ising model, used for understanding diffusive phase separation as in solid mixtures, in  $d = 2$  (on regular square lattice) and  $d = 3$  (on simple cubic lattice), via extensive simulations, to quantify the decay of  $C(t, t_w)$ . We observe scaling of  $C(t, t_w)$  with respect to  $x$  in which the power-law of Eq. (2) is realized for large  $x$ . Via computations of the instantaneous exponent [21–23]

$$\lambda_i = -\frac{d \ln[C(t, t_w)]}{d \ln x}, \quad (7)$$

and application of the finite-size scaling technique [24, 25], we find that  $\lambda \simeq 3.6$  in  $d = 2$  and  $\simeq 7.5$  in  $d = 3$ . Though these numbers respect the bounds in Eq. (4), the high value in  $d = 3$  is surprising. But this comes from both CH and Ising models, from various reliable analyses. Furthermore, a general analytical form for the full scaling functions has been obtained empirically.

## II. METHODS

One numerically solves the CH equations on a regular lattice, usually via Euler discretization method. With the Ising model, phase separation kinetics in a solid binary mixture is studied via the Kawasaki exchange Monte Carlo (MC) [25] simulations, to be referred to as KIM. An up spin ( $S_i = +1$ ), for this problem, may correspond to an  $A$  particle and a down spin ( $-1$ ) to a  $B$  particle. In this MC scheme, one randomly chooses a pair of nearest neighbor spins and tries their position exchange. The moves are accepted according to standard Metropolis algorithm [25]. Due to the coarse-grained nature of the CH equation, as opposed to the atomistic Ising model, one can explore large effective length in simulations. The order parameter in Eq. (5) corresponds to a coarse-graining [26] of the Ising spins, typically over the equilibrium correlation length  $\xi$ . Then, a positive value of  $\psi$  means an  $A$ -rich region and for a  $B$ -rich region,  $\psi$  will have a negative number. For the calculation of  $C(t, t_w)$ , we have used binary numbers  $+1$  and

-1, for both the models.

The average domain length,  $\ell$ , in our simulations was measured from the first moment of domain size distribution,  $P(\ell_d, t)$ , as [23]

$$\ell = \int \ell_d P(\ell_d, t) d\ell_d, \quad (8)$$

where  $\ell_d$  is the distance between two successive domain boundaries in any direction. Throughout the paper, all lengths are presented in units of the lattice constant  $a$ . In MC simulations, time is counted in units of Monte Carlo steps (MCS), each MCS consisting of  $L^d$  trial moves, where  $L$  is the linear dimension of a periodic square or cubic system. In CH equation,  $t$  is expressed dimensionless units [27]. All results are presented after averaging over at least 50 initial configurations, for quenches from random initial configurations to  $T = 0.6T_c$ .

### III. RESULTS

In Fig. 1(a), we present the plots of  $C(t, t_w)$ , vs  $x$ , for different values of  $t_w$ , from the solutions of CH model in  $d = 2$ . As seen, one needs large enough value of  $t_w$  to observe appropriate scaling behavior, compared to ordering in ferromagnets [14]. Between the two data sets with largest values of  $t_w$ , the deviation from each other, for large  $x$ , is due to the finite-size effects. Similar plots for the  $d = 3$  CH model are presented in Fig. 1(b). Here all  $t_w$ s are large enough, providing good scaling. Again, deviation from the master curve, starting at different values of  $x$  for different  $t_w$ , are primarily related to the finite-size effects. In both these figures, 1(a) and 1(b), the system sizes are kept fixed, only the values of  $t_w$  are varied. A similar observation, with respect to the above mentioned deviation for different choices of  $t_w$ , can be made, when, for same value of  $t_w$ , data are presented for different system sizes.

In the scaling parts, both in Fig. 1(a) and Fig. 1(b), continuous bending is observable, in these log-log plots. Thus, power-laws, if exist, carry corrections. The solid lines in these figures

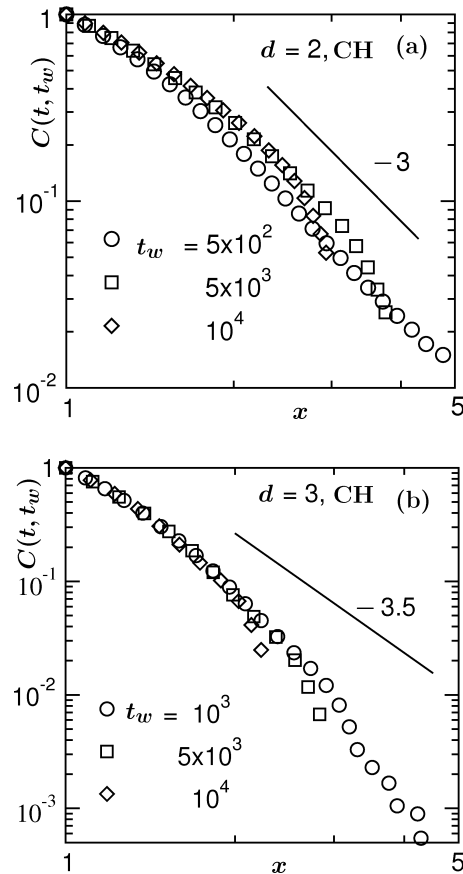


FIG. 1. (a) Autocorrelation function,  $C(t, t_w)$ , from the  $d = 2$  Cahn-Hilliard model, are plotted vs  $x$  ( $= \ell/\ell_w$ ), for different values of  $t_w$ . The solid line there corresponds to a power-law decay with exponent 3. (b) Same as (a) but for the  $d = 3$  CH model. The solid line there has a power-law decay exponent 3.5. The system sizes used are  $L = 256$  ( $d = 2$ ) and  $200$  ( $d = 3$ ).

are power-law decays with exponents 3 and 3.5, respectively, corresponding to the bounds in Eq. (4). For large  $x$ , simulation data in  $d = 2$  appear reasonably consistent with the bound. The asymptotic exponent, in  $d = 3$ , on the other hand, appear much higher than 3.5.

With the expectation that power laws indeed exist, in Fig. 2 we present plots of instantaneous exponents [6, 14, 21–23]  $\lambda_i$ , for both  $d = 2$  and 3, vs  $1/x$ . In addition to providing  $\lambda$ , from the extrapolations to  $x = \infty$ , such exercise may be useful for obtaining crucial information on the full forms of  $C(t, t_w)$ . For  $d = 2$ , the data are obtained for  $t_w = 5 \times 10^3$ , and for  $d = 3$ , the data correspond to  $t_w = 10^3$ . In both the cases, the results appear reasonably linear [6, 14].

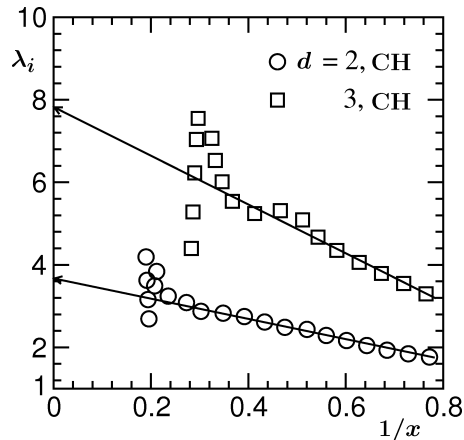


FIG. 2. Instantaneous exponents  $\lambda_i$  are plotted vs  $1/x$ . Results are shown only from the solutions of the CH equations, in both  $d = 2$  and 3. The solid lines are guides to the eye. The  $d = 2$  data are for  $t_w = 5 \times 10^3$  with  $L = 400$ . In  $d = 3$  the numbers are  $10^3$  and 200.

The solid lines there are extrapolations to  $x = \infty$ , accepting the linear trends. These indicate  $\lambda \simeq 3.60$  in  $d = 2$  and  $\simeq 7.80$  in  $d = 3$ . Again, while the value in  $d = 2$  is consistent and close to the bound of Yeung [7] et al., the observation of surprisingly high number in  $d = 3$  is certainly interesting. We intend to obtain more accurate values via appropriate finite-size scaling analyses [24, 25]. This is considering the fact that the choice of the regions in Fig. 2, for performing least-square fitting, is not unambiguous due to finite-size effects and strong statistical fluctuations at large  $x$ . Also, for very small  $x$  (data excluded), there is rapid decay of  $C(t, t_w)$  related to the fast equilibration of domain magnetization.

Since the corrections to the asymptotic decay laws are seen to be strong for finite  $x$ , a reasonable idea about the full forms of the decays is essential for accurate finite-size scaling analyses. Those, however, are nonexistent in the literature. Here we obtain the forms empirically. Assuming power-law behavior of the data sets in Fig. 2, we write

$$\lambda_i = \lambda - \frac{A_c}{x^\gamma}, \quad (9)$$

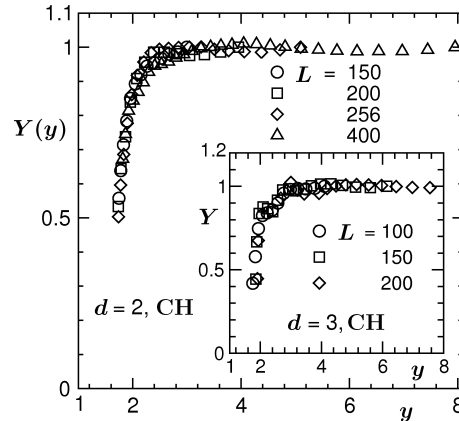


FIG. 3. Finite-size scaling plot of  $C(t, t_w)$  from  $d = 2$  CH model. The scaling function  $Y$  is plotted vs  $y$ , using data from different system sizes. The optimum collapse of data, the presented one, was obtained for  $\lambda = 3.47$ . The inset presents the same exercise for the CH model in  $d = 3$ . Here the value of  $\lambda$  is 7.30. See text for values of  $t_w$ .

where  $A_c$  and  $\gamma$  are constants. Combining Eq. (9) with Eq. (7), we obtain

$$C(t, t_w) = C_0 \exp\left(-\frac{A_c}{\gamma x^\gamma}\right) x^{-\lambda}, \quad (10)$$

$C_0$  being a constant. For finite-size scaling analysis, one needs to introduce a scaling function

$$Y(y) = C(t, t_w) \exp\left(\frac{A_c}{\gamma x^\gamma}\right) x^\lambda; \quad y = L/\ell. \quad (11)$$

For appropriate choices of  $A_c$ ,  $\gamma$  and  $\lambda$ , one should obtain a master curve for  $Y$ , when data from different system sizes are used. The behavior of  $Y$  should be flat in the finite-size unaffected region and a deviation from it will mark the onset of finite-size effects.

By examining the data in Fig. 2 (also see Fig. 4(b) for KIM), we fix  $\gamma$  to 1. In the main frame of Fig. 3, we show a finite-size scaling plot for data from the  $d = 2$  CH model. The presented results correspond to best collapse, obtained for  $A_c = 2.25$  and  $\lambda = 3.47$ . The value of  $t_w$  used for all the data sets is  $10^4$ . A similar exercise for the  $d = 3$  CH data is presented in the inset of Fig. 3. Again the data collapse looks quite reasonable and was obtained for  $A_c = 5.1$  and  $\lambda = 7.30$ . The value of  $t_w$ , in this case, was set to  $10^3$ . The reason behind

choosing smaller value of  $t_w$  in  $d = 3$ , than in  $d = 2$ , is computational difficulty. It is extremely difficult to accumulate data for further decades in time, starting from very high value of  $t_w$ , particularly in  $d = 3$ . Nevertheless, this chosen value of  $t_w$  falls within the scaling regime. Note that for similar temperatures, amplitude of growth is larger in  $d = 3$  and the scaling of  $C(t, t_w)$  is related more closely to the value of  $\ell_w$ . In this connection we mention that the longest run lengths (associated with largest systems) for the CH model are  $t = 2 \times 10^6$  and  $2 \times 10^5$  in  $d = 2$  and 3, respectively; for the Ising model these numbers are  $5 \times 10^7$  and  $4 \times 10^6$ .

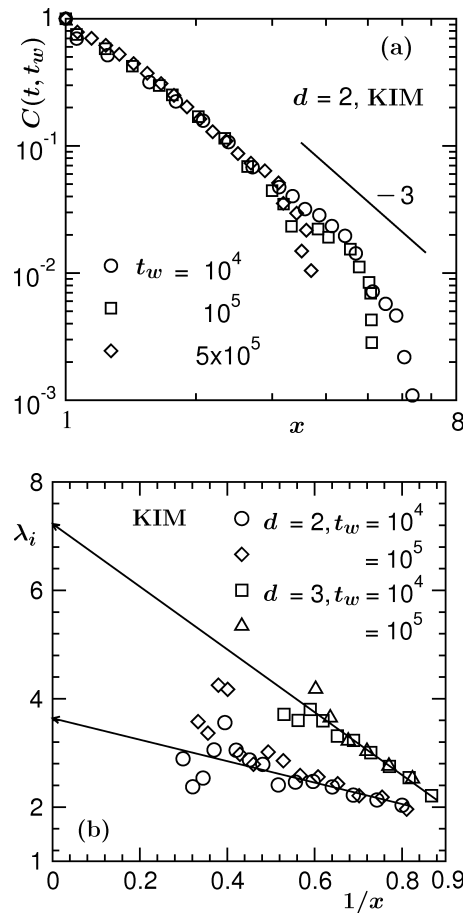


FIG. 4. (a) Same as Fig. 1(a) but for the  $d = 2$  Ising model. (b) Same as Fig. 2 but for Ising model. The oscillatory behavior of large  $x$  data in  $d = 2$  is statistical fluctuation. In  $d = 2$  the results are from  $L = 512$  and in  $d = 3$ , we have used  $L = 100$ .

We now move to present results from KIM. In Fig. 4(a) we show the autocorrelations from

different values of  $t_w$  in  $d = 2$ , for  $L = 512$ . Scaling is poor for  $t_w$  below  $10^4$  MCS and so those results are excluded. Despite strong statistical fluctuations, it is recognizable that the decay of  $C(t, t_w)$  in the latter part is on the higher side of the bound in Eq. (4), represented by the solid line.

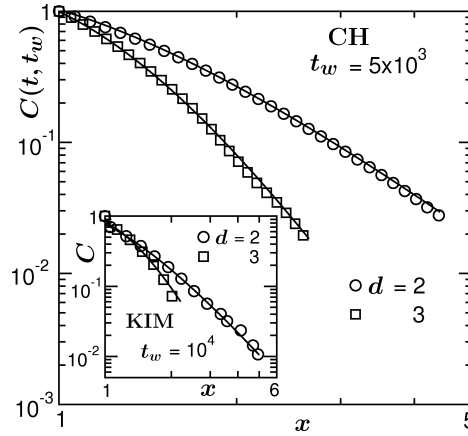


FIG. 5.  $C(t, t_w)$  are plotted vs  $x$ , for the CH model in  $d = 2$  and 3. Inset shows corresponding results for the KIM. The solid lines are fits to the form in Eq. (10), with  $\gamma = 1$ . The  $t_w$  values are mentioned on the figure. We have discarded data suffering from finite-size effects. The system sizes are  $L = 400$  and 512 for CH and Ising models in  $d = 2$ , whereas,  $L = 200$  and 100 in  $d = 3$ .

In Fig. 4(b) we show the instantaneous exponents for the Ising model in  $d = 2$  and 3, vs  $1/x$ . In each dimension, we have included two values of  $t_w$  from the scaling regime. While results for different  $t_w$ s, in a particular dimension, are consistent with each other, finite-size effects appear earlier for larger value of  $t_w$ , as expected. Thus, for extrapolations to  $x = \infty$ , data sets with smaller  $t_w$  are used. This exercise provides  $\lambda \simeq 3.60$  and  $\simeq 7.30$  in  $d = 2$  and 3, respectively. These values are in agreement with the ones obtained for the CH model via various methods of analysis.

Finally, in Fig. 5 we show the fits of the simulation data to the form in Eq. (10). The main frame is for the CH model in  $d = 2$  and 3, whereas the inset contains similar results from the

KIM. The fits look quite satisfactory. This exercise provides  $\lambda = 3.55$  and  $3.76$  in  $d = 2$  for CH and Ising models, respectively. The numbers in  $d = 3$  are  $7.64$  and  $7.37$ .

#### IV. CONCLUSIONS

In conclusion, we have studied aging dynamics for the phase separation in solid binary mixtures via Cahn-Hilliard and Ising models. Results for the two-time autocorrelation,  $C(t, t_w)$ , are presented from simulations in both  $d = 2$  and  $3$ . Decays of  $C(t, t_w)$  appear power law in large  $x$  limit. The exponents for these power laws were obtained via various different analyses, including finite-size scaling, which is new for this purpose. For the finite-size scaling analysis, full forms of the autocorrelations were essential which we obtained empirically. All these methods provide consistent values of the decay exponent  $\lambda$  for different models. These are  $\lambda \simeq 3.6$  in  $d = 2$  and  $\lambda \simeq 7.5$  in  $d = 3$ , within 5% error.

Very high value of  $\lambda$  in  $d = 3$ , far above the lower bound in Eq. (4), can be due to the fact that domains are more mobile in this dimension than in  $d = 2$ . From the numbers obtained in  $d = 2$  and  $3$ , it may be tempting to predict a dimensionality dependence as  $\lambda = f(d - 1)$  with  $f \simeq 3.75$ . However, we caution the reader not to jump into such conclusion. Even though the influence of the dimension  $d$  appear more important than in the bound of Eq. (4), the contribution of  $\beta$  is significant, particularly at lower dimension. Results from other dimensions are necessary to make such a conclusion. In  $d = 1$  one should exercise the caution that  $\beta (= 2)$  has a different value[28].

## V. ACKNOWLEDGMENT

The authors acknowledge financial support from Department of Science and Technology, India, via Grant No SR/S2/RJN-13/2009. JM is grateful to the University Grants Commission for research fellowship and SM acknowledges Jawaharlal Nehru Centre for Advanced Scientific Research for financial support.

\* das@jncasr.ac.in

- 
- [1] *Kinetics of Phase Transitions*, edited by S. Puri and V. Wadhawan (CRC Press, Boca Raton, 2009).
- [2] R.M.Z. dos Santos and A.T. Bernardes, Phys. Rev. Lett. **81**, 3034 (1998).
- [3] M. Costa, A.L. Goldberger and C.-K. Peng, Phys. Rev. Lett. **95**, 198102 (2005).
- [4] D.S. Fisher and D.A. Huse, Phys. Rev. B, **38**, 373 (1988).
- [5] G.F. Mazenko, Phys. Rev. B **42**, 4487 (1990).
- [6] F. Liu and G.F. Mazenko, Phys. Rev. B **44**, 9185 (1991).
- [7] C. Yeung, M. Rao and R.C. Desai, Phys. Rev. E **53**, 3073 (1996).
- [8] G.F. Mazenko, Phys. Rev. E **69**, 016114 (2004).
- [9] J.F. Marko and G.T. Barkema, Phys. Rev. E **52**, 2522 (1995).
- [10] S. Puri and D. Kumar, Phys. Rev. Lett. **93**, 025701 (2004).
- [11] S. van Gemmert, G.T. Barkema and S. Puri, Phys. Rev. E **72**, 046131 (2005).
- [12] S. Ahmad, F. Corberi, S.K. Das, E. Lippiello, S. Puri and M. Zannetti, Phys. Rev. E **86**, 061129 (2012).
- [13] S. Majumder and S. K. Das, Phys. Rev. Lett. **111**, 055503 (2013).
- [14] J. Midya, S. Majumder and S.K. Das, J. Phys.: Condens. Matter, **26**, 452202 (2014).

- [15] B. Abou and F. Gallet, Phys. Rev. Lett. **93**, 160603 (2004).
- [16] G.G. Kenning, G.F. Rodriguez and R. Orbach, Phys. Rev. Lett. **97**, 057201 (2006).
- [17] L. Berthier, Phys. Rev. Lett. **98**, 220601 (2007).
- [18] E. Buchbinder and J.S. Langer, Phys. Rev. E **83**, 061503 (2011).
- [19] J. Bergli and Y.M. Galperin, Phys. Rev. B **85**, 214202 (2012).
- [20] A.J. Bray, Adv. Phys. **51**, 481 (2002).
- [21] D.A. Huse, Phys. Rev. B, **34**, 7845 (1986).
- [22] J. G. Amar, F. E. Sullivan and R. D. Mountain, Phys. Rev. B **37**, 196 (1988).
- [23] S. Majumder and S.K. Das, Phys. Rev. E **81**, 050102 (2010).
- [24] M. E. Fisher in *Critical Phenomena*, edited by M.S. Green (Academic Press, London, 1971).
- [25] D.P. Landau and K. Binder, *A Guide to Monte Carlo Simulations in Statistical Physics*, Cambridge University Press, 3rd Edition (2009).
- [26] A. Onuki, *Phase Transition Dynamics* (Cambridge University Press, Cambridge, 2002).
- [27] K. Binder, S. Puri, S.K. Das and J. Horback, J. Stat. Phys. **73**, 182 (1994).
- [28] S.N. Majumdar, D. A. Huse and B.D. Lubachevsky, Phys. Rev. Lett. **138**, 51 (2010).